Chinese Chemical Letters 34 (2023) 107562

Contents lists available at ScienceDirect

Chinese Chemical Letters

journal homepage: www.elsevier.com/locate/cclet

Perpyrrospirone A, an unprecedented hirsutellone peroxide from the marine-derived *Penicillium citrinum*

Yi Ding, Yu Jiang, Sunjie Xu, Xiujuan Xin, Faliang An*

State Key Laboratory of Bioreactor Engineering, East China University of Science and Technology, Shanghai 200237, China

ARTICLE INFO

Article history:
Received 5 January 2022
Revised 20 May 2022
Accepted 23 May 2022
Available online 27 May 2022

Keywords:
Penicillium citrinum
Hirsutellone
Peroxide
X-ray
Cytotoxicity

ABSTRACT

Perpyrrospirone A (**1**) characterized an unprecedented 6/5/6/8/5/13/6 oxahexacyclic scaffold with a unique peroxide-bridged 8,9-dioxa-2-azaspiro[4.7]dodecane core from marine-derived *Penicillium citrinum*. Compounds **2** and **3** possessed rare oxatetracyclic (6/5/6/5) skeleton fused with a 13-menbered-ring macrocyclic moiety. Their structure and absolute configurations were determined by comprehensive spectroscopic analyses, ECD data coupled with TD-DFT calculations and X-ray diffraction experiments. In addition, **7** showed cytotoxicity and induced apoptosis of Hela cells in a dose-dependent manner after a 48 h treatment.

The natural hirsutellone family products are made of a decahydrofluorene polyketide core (rings A, B and C) involved in a highly strained 12- or 13-membered *para*-cyclophane (ring D) and highly functionalized 5-hydroxypyrrolidinone (Fig. S1 in Supporting information) [1]. The various ring junctions and chiral centers generated the diverse structures, at the meantime, giving a rise to the multiple and fascinating biological activities, such as cytotoxicity, anti-tuberculosis activity, and antifungal activity [2]. The unique feature and diverse bioactivity of hirsutellone family has attracted significant interest from biosynthetic, synthetic chemists and pharmacologists [3–7]. Up to now, a total of 44 compounds of this type had been discovered from various fungi, categorized into thirteen carbon skeletons (Fig. S1). Among these isolates, 15 of them were isolated from the genus *Penicillium*, including the tricyclic decahydroflu-orene (6/5/6) skeleton analogues (GKK1032s A-C) [1–7], the series of cyclohexano[α]decahydrofluoren (6/5/6/6) framework (pyrrospirones C-I), the rare 6/5/6/5 fused ring system (pyrrospirone J and penicipyrroether A), and the unique adduct (penicipyrrodiether A) [8–11].

Dereplication is an essential step in the natural product workflow to minimize the reevaluation of know compounds and expedite the discovery process [12]. Recently, the mass spectrometry-based molecular networking (MN) has emerged as a promising analysis technique to visualize and organize the tandem MS/MS data set within complex mixtures [13]. The fundamental principle of MN is that structurally related molecules possess similar MS/MS fragmentation patterns and should be categorized into a subnetwork according to similar scaffolds [14]. This dereplication strategy identified both known compounds and potential related new analogues, thereby prioritized the isolation towards undiscovered molecules [15]. Accordingly, as a continuation of our search for novel bioactive compounds from marine-derived fungi, MN was conducted in order to accelerate the discovery rate of new molecules with specific structural features from the endophytic strain *P. citrinum* DY180712, leading to the isolation of seven new hirsutellone analogues, together with nine known compounds **8**–**16** (Fig. 1, Figs. S1 and S2 in Supporting information) [1–7]. To our knowledge, perpyrrospirone A (**1**) was the first hirsutellone peroxide featuring an unprecedented 2,3-peroxide-bridged oxatetracyclic (6/5/6/8) skeleton. Herein, we reported the isolation, structural identification and bio-evaluation of isolated compounds.

Perpyrrospirone A (**1**) was obtained as colorless crystals, and its molecular formula was assigned to be $C_{32}H_{41}NO_8$ by HRESIMS data (m/z 568.2902 $[M+H]^+$) and interpretation of the ^{13}C NMR data, indicating 13° of unsaturation. The ^1H NMR data (Table S1 in Supporting information) displayed three exchangeable protons at 8.13 (s), 6.65 (d, $J = 6.0$ Hz) and 5.97 (s), four *para*-substituted aromatic protons at δ_H 7.00 (dd, $J = 8.6$, 2.1 Hz), 6.68 (dd, $J = 8.6$, 2.5 Hz), 6.62 (dd, $J = 8.1$, 2.5 Hz) and 7.09 (dd, $J = 8.1$, 2.1 Hz), and five methyl groups at δ_H 1.22 (s), 1.28 (s), 1.44 (s), 0.88 (d, $J = 0.88$, 6.3 Hz) and 1.00 (d, $J = 6.1$ Hz). The 32 carbon signals in the ^{13}C NMR data (Table S2 in Supporting information) were assigned with the help of the DEPT and HSQC experiments, indicating the presence of five

---

[*] Corresponding author.
E-mail address: flan2016@ecust.edu.cn (F. An).

https://doi.org/10.1016/j.cclet.2022.05.076

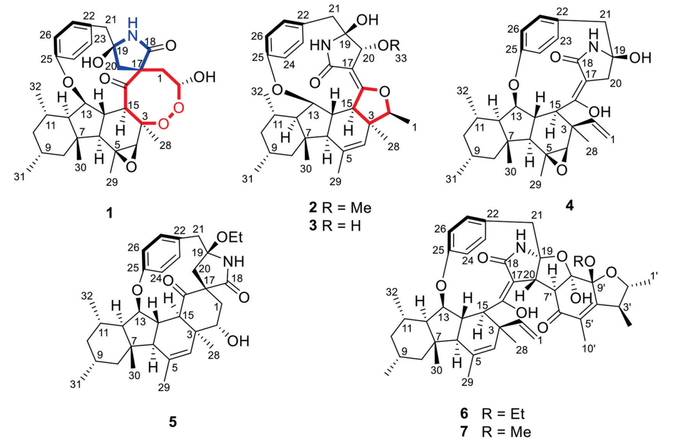

Fig. 1. Structures of compounds **1**–**7**.

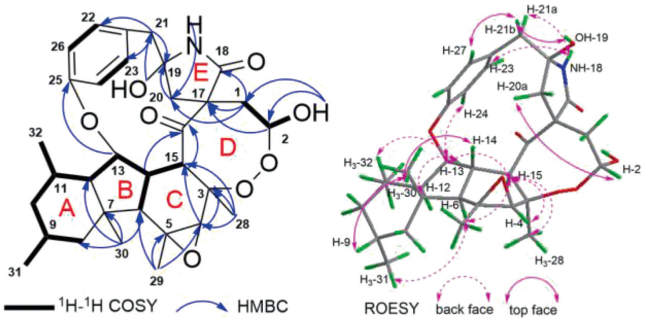

Fig. 2. Key ^{1}H–^{1}H COSY, HMBC and ROESY correlations of **1**.

methyl groups, five methylenes, 13 methines and 9 nonprotonated carbons.

The planar structure of **1** was established by extensive 2D NMR spectra (Fig. 2). Detailed analyses of the ^{1}H–^{1}H COSY data revealed the partial structure shown as bold lines, along with the HMBC correlations from the methyl group H_3–30 to C-6, C-7, C-8 and C-12, from H_3–29 to C-4, C-5 and C-6, from H_3–28 to C-3, C-4 and C-15, and from H-4 to C-15, constructed a tricyclic system (rings A/B/C) with five methyl groups for compound **1**. Further cross-peaks from H-14 to C-16, from H-2 to C-17, and from H-1 to C-18 and C-20, as well as the down field shifted C-2 (δ_C 96.3) and C-3 (δ_C 84.6), indicated a multiple oxygen ring attached at C-3 and C-15 in the C ring and C-17 in the D ring [9]. The observed HMBC correlations from NH-18 to C-17, C-18, C-19 and C-20, and from 19-OH to C-20 implied the presence of a γ-lactam moiety. The cross-peaks from H_2–21 to C-19, C-23 and C-27 allowed the connection of the *para*-disubstituted aromatic ring to this γ-lactam moiety *via* a methylene. The HMBC correlation of H-13/C-25, as well as the de-shielded C-13 (δ_C 88.4) and C-25 (δ_C 157.6), implied an ether linkage between C-13 and C-25. To satisfy the remaining degree of unsaturation, one epoxy ring attached at C-4/C-5 was required, which was supported by typical upfield oxygen-bearing ^{13}C NMR chemical shifts (δ_C 64.8 and 54.7) and the cross-peaks from H_3–29 to C-4 and C-6. Thus, the planar structure of **1** was established as shown.

The relative configuration of **1** was established by analysis of key ROESY correlations (Fig. 2). The key correlations of H-24 with H-13, H-13 with H-12, H-15 and H_3–32, H-15 with H-4 and H_3–28, H-6 with H_3–31, and NH-18 with H-23 and H-21a assigned all these protons to be α-oriented and determined the relative configuration of the spirocarbon (C-17) as shown. The vicinal coupling constant of $J_{6,14} = 12.9$ Hz and cross-peaks of H-14 with H_3–30, H_3–30 with H-9, H-27 with H-21β, H-21β with OH-19, and OH-19 with OH-2 implied that they were positioned on the other face, *i.e.* β-oriented. Thus, the relative configuration of compound **1** was determined to be 2*R**, 3*R**, 4*S**, 5*S**, 6*R**, 7*R**, 9*R**, 11*S**, 12*R**, 13*S**, 14*S**, 15*R**, 17*R** and 19*R**. Subsequently, the planar structure and absolute configuration of **1** were assigned to be 2*R*, 3*R*, 4*S*, 5*S*, 6*R*, 7*R*, 9*R*, 11*S*, 12*R*, 13*S*, 14*S*, 15*R*, 17*R*, and 19*R* by well agreement between the calculated and measured ECD data (Fig. 3A and Fig. S3 in Supporting information) and an X-ray single crystal diffraction experiment with Flack parameter of 0.04 (9) (Cu Kα, CCDC: 2092966, Fig. 3B). Thus, **1** was unambiguously elucidated as a hirsutellone alkaloid possessing unprecedented 6/5/6/8/5/13/6 oxahexacyclic scaffold with an unique peroxide-bridged 8,9-dioxa-2-azaspiro[4.7]dodecane core and named perpyrrospirone A.

Penicillione B (**2**) and penicillione C (**3**) were obtained as white powder, and their molecular formulas were determined to be $C_{33}H_{43}NO_5$ and $C_{32}H_{41}NO_5$ on the basis of high-resolution HR-ESI-MS data (*m/z* 534.3212 $[M+H]^+$, calcd. 534.3214) and (*m/z* 542.2874 $[M+Na]^+$, calcd. 542.2877), respectively. The ^{1}H NMR, ^{13}C NMR and DEPT data (Tables S1 and S2) assigned the existence of seven rings in **2**. The spin systems from H-8 to H-15, from H-6 to H-14, and from H_3–1 to H-2 were deduced from COSY correlations. HMBC correlations (Fig. S4 in Supporting information) from H_3–30 to C-6, C-7, C-8 and C-12, from H3–29 to C-4, C-5 and C-6, from H_3–28 to C-2, C-3, C-4 and C-15, from H-4 to C-6 and C-15, and from H-2 to C-16, revealed that **2** had a 6/5/6/5 oxatetracyclic skeleton, similar to penicipyrroether A. Instead of the hemiketal group at C-16, the double bond of C16-C17 in **2** was found to link to the γ-lactam moiety based on HMBC correlations from H-2 to C-16, H-20 to C-16, and NH-18 to C-17. The correlations from H_3–33 to C-20, and from H-20 to C-18 and C-21 located a methoxy

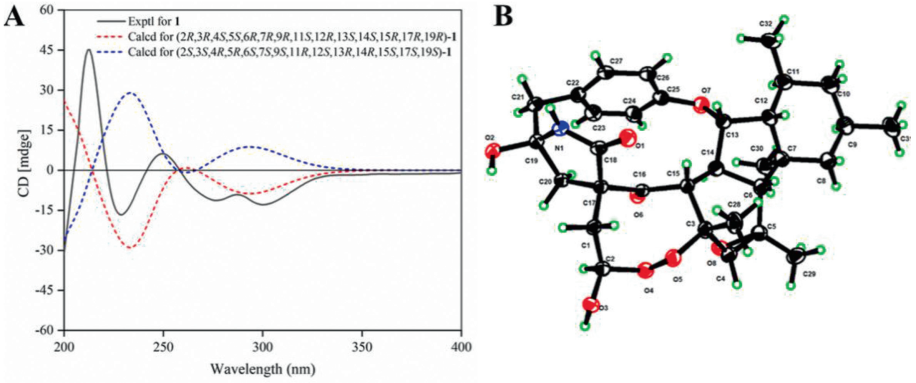

Fig. 3. (A) Experimental and calculated ECD spectra of **1**. (B) X-ray ORTEP diagram of **1**.

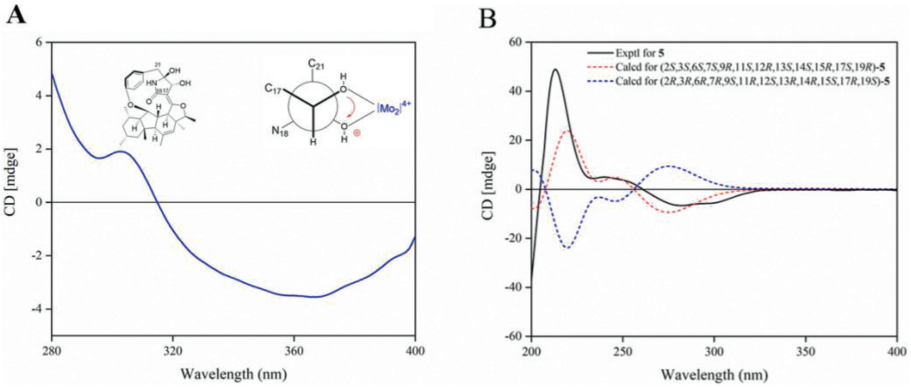

Fig. 4. (A) $Mo_2(OAc)_4$-induced ECD spectra of **3**. (B) Experimental and calculated ECD spectra of **5**.

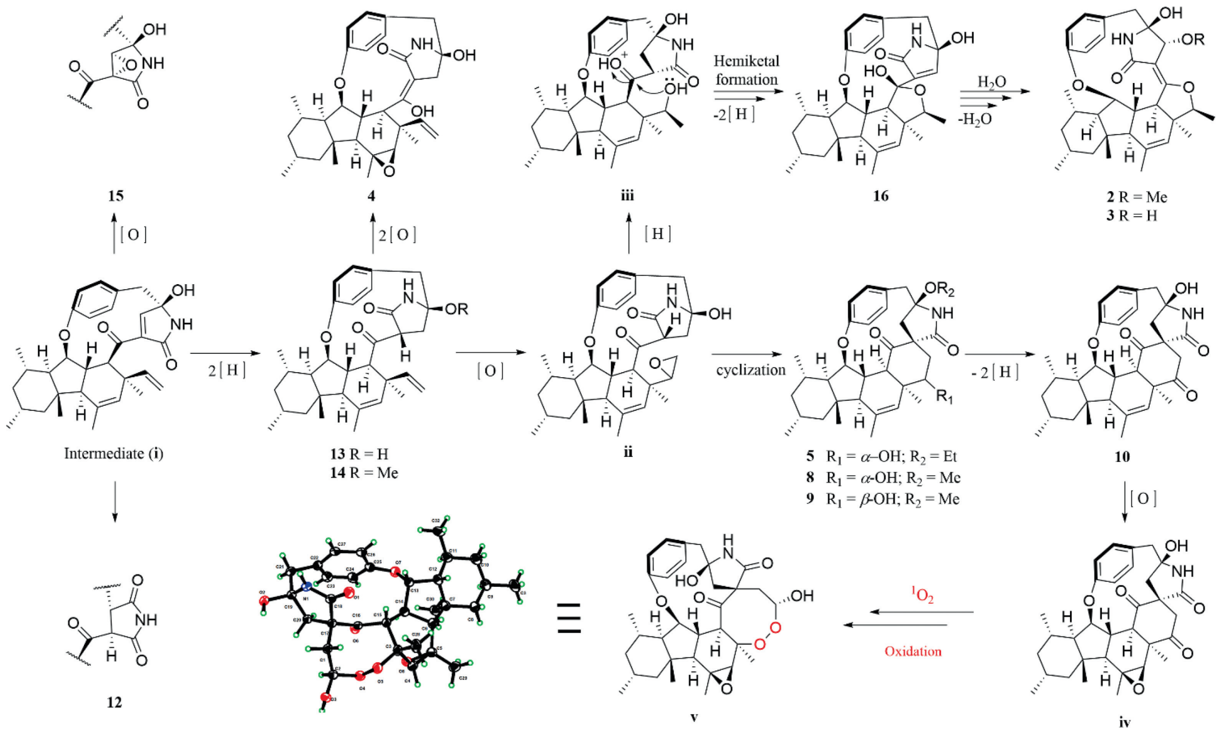

Scheme 1. Plausible biosynthetic pathway of the new compound **1**.

group at C-20. The relative configuration of **2** was determined by analysis of the ROESY data. Two double bonds of $\Delta^{4,5}$ and $\Delta^{16,17}$ were determined to be in *Z*- and *E*-geometry based on the ROE cross-peaks of H-4 with H_3–29 and H-2 with H_3–22, respectively. The key ROE correlations of H-27 with H-21b and H-20, H-21b with OH-19, H-26 with H-14, H-14 with H_3–30 and H_3–1 indicated a β-orientation for all these protons. Additional ROE correlations of H-23 with H-21a, H-24 with H-13 and H_3–32, H_3–32 with H_3–31, H-13 with H-12 and H-15, H-15 with H_3–28 and H-6, and H-2 with H_3–33 revealed they were positioned on the other face. The ^1H and ^{13}C data of **3** (Tables S1 and S2) were similar to those of **2** revealing a CH_2 unit in **3** < **2**. Careful comparison of the NMR data of **3** with those of **2**, suggested **3** was a 20-demethoxy derivative of **2**. The final planar structure and relative configuration of **3** were established by detailed 2D NMR data analysis as shown (Figs. S4, S30 and S32 in Supporting information). In addition, the ECD data of **3** (Fig. S26 in Supporting information) was also in accordance with **2**. The absolute configurations of C-19 and C-20 were determined *via* $Mo_2(OAc)_4$-induced ECD classical method developed by Snatzke [16–18]. The positive Cotton effect at 306 nm suggested that C-19 and C-20 were *S* and *R* configurations (Fig. 4A), respectively. Thus, compounds **2** and **3** possessed rare oxatetracyclic (6/5/6/5) skeleton fused with a 13-menbered-ring macrocyclic moiety, and the absolute configurations of compounds **2** and **3** were defined as 1*S*, 3*S*, 6*S*, 7*S*, 9*R*, 11*S*, 12*R*, 13*S*, 14*S*, 15*R*, 19*S* and 20*R*.

Penicillione D (**4**) was isolated as a white solid. Its molecular formula was determined to be $C_{32}H_{41}NO_5$ on the basis of HRESIMS (*m/z* 542.2875 $[M+Na]^+$, calcd. 542.2877) and ^{13}C NMR data, corresponding to 13° of unsaturation. The NMR data of **4** were similar to those of **13**, except for one oxygenated methine (δ_C 65.9, δ_H 2.83 s) and three quaternary carbons (δ_C 65.9, 105.4 and 158.2). Furthermore, the disappearance of the ketone carbonyl group at C-16 and the methine at C-17, and the presence of an exchangeable signal OH-16 (δ_H 7.23) in **4**, suggested that there was a rare enol motif between C-16 (δ_C 158.2) and C-17 (δ_C 105.4), which was supported by the HMBC correlations from H-15 to C-16 and C-17, and

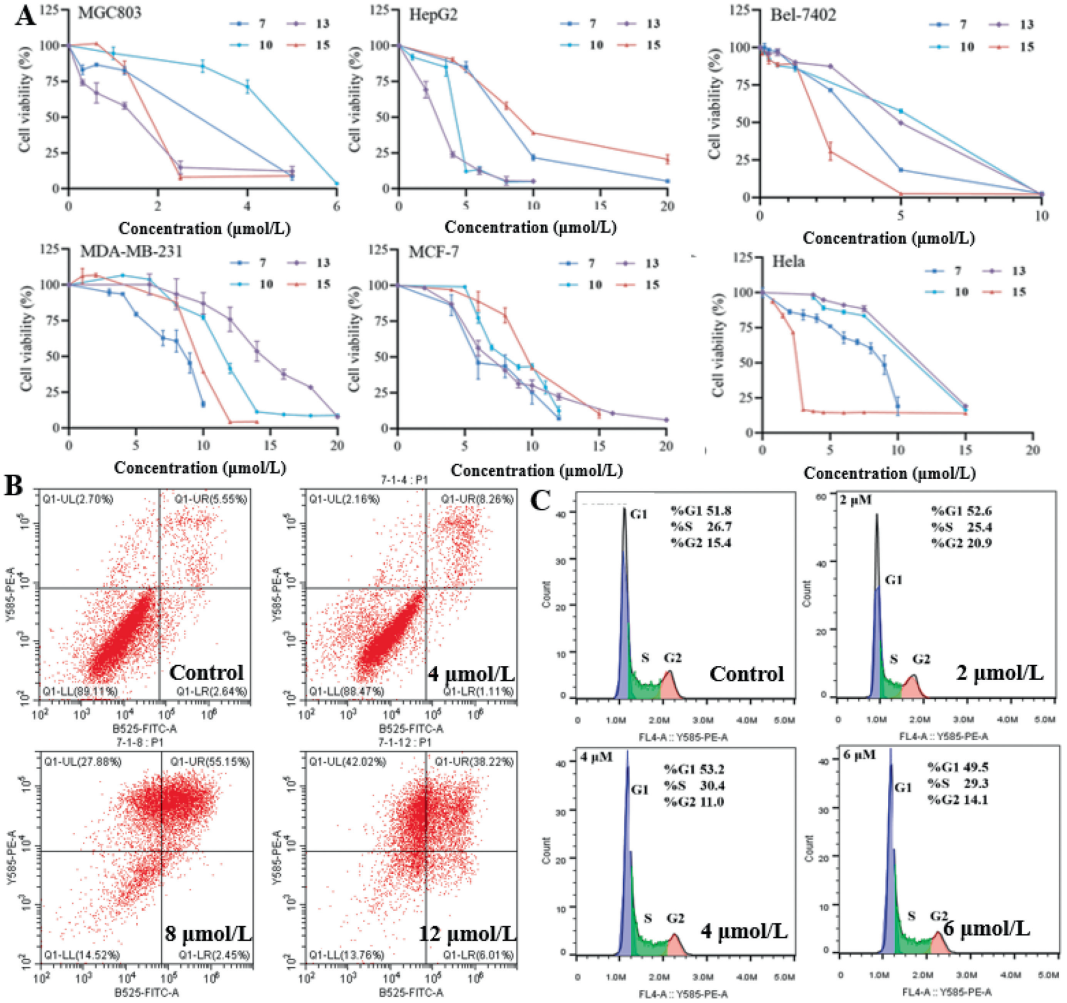

Fig. 5. (A) Dose-response viability curves for six cancer cell lines after treatment for 48 h. (B) Flow cytometric analysis of apoptosis stained with Annexin V-FITC and PI. HeLa cells were untreated or treated with 4, 8 and 12 μmol/L compound **7** for 48 h. (C) Cell cycle in HeLa cells untreated or treated with **7** for 24 h.

from H-20 to C-16, C-17, C-18, C-19 and C-21 (Fig. S4). Moreover, two characteristic oxygenated carbons (δ_C 65.9 and 62.6) in **4** instead of the olefinic carbons in compound **13** indicated the presence of an epoxide group between C-4 and C-5, which was further confirmed by the HMBC correlations from H_3–29 to C-4, C-5 and C-6, from H-15 to C-4, and from H-2 to C-4 (Fig. S4). The relative configuration of **4** was elucidated on the basis of the ROESY data (Fig. S5 in Supporting information, measured in DMSO-d_6). The absolute configuration of **4** was defined by the good agreement between the calculated and measured ECD and assigned a (3*R*, 4*R*, 5*S*, 6*R*, 7*R*, 9*R*, 11*S*, 12*R*, 13*S*, 14*R*, 15*R* and 19*S*)-configuration to **4**.

Penicillione E (**5**), a white powder, had a molecular formula of $C_{34}H_{45}NO_5$ determined by the HR-ESI-MS *pseudo* molecular ion peak at 570.3188 $[M+Na]^+$, a CH_2 unit more than **8**. Spectroscopic analyses of its UV and 1D NMR suggested that **5** was an analogue of pyrrospirone D (**8**) [8–11]. Careful comparison of the NMR data between **5** and **8** indicated that their structural difference was that the methoxy group at C-19 in **5** was replaced by an ethoxy group (δ_H 3.51, m and 1.22, t, $J = 7.1$ Hz; δ_C 58.3 and 15.9). The final planar structure of **5** was established by detailed 2D NMR data analysis as shown (Figs. S4 and S5). The configuration at C-2 was determined by comparing the ^1H NMR chemical shift and the coupling pattern for H-2 with those of pyrrospirones C and D (**8** and **9**): The configuration of H-2 (δ_H 2.73, m) in **5** was the same as that in **8** (δ_H 2.74, m) other than in **9** (δ_H 4.43, dd, $J = 11.3$, 5.3 Hz). In addition, comparison of the experimental ECD spectra of these compounds revealed that the absolute configurations of **5** were identical to **8** as 2*S*, 3*S*, 6*S*, 7*S*, 9*R*, 11*S*, 12*R*, 13*S*, 14*S*, 15*R*, 17*S*, 19*R*, which was also confirmed by experimental and calculated ECD data using TD-DFT at the B3LYP/6–31+g(d, p) level (Fig. 4).

Penicillione F (**6**), white crystals, had a molecular formula to be $C_{45}H_{57}NO_8$. The ^1H and ^{13}C NMR spectra of **6** closely resembled those of **11**, except for the absence of a hydroxy group and presence of an additional ethoxy group signals (δ_H 3.33, m, 3.63, m; δ_H 1.17, t, $J = 6.9$ Hz). Analysis of the ROESY data suggested that **6** shared the same relative configuration as **11** (Fig. S5). Single crystals were acquired in methanol, and the planar structure and absolute configuration of **6** were established by single-crystal X-ray diffraction analysis on the Cu Kα data (CCDC: 2043219, Fig. S6 in Supporting information) with Flack parameter of 0.06 (13), allowing an assignment of the absolute configurations as shown. Penicillione G (**7**) had the molecular formula $C_{44}H_{55}NO_8$, a CH_2 unit less than that of **6**. Its 1D NMR data were similar to those of **6**, except for the replacement of the ethoxy group in **6** with an methoxy group (δ_H 3.30, s; δ_C 51.1) in **7**. Detailed analysis of the 2D NMR spectra of **7** indicated that the remaining structural units were identical to those of **6**. The relative configuration of **7** was resolved by similar key ROE correlations compared with **6**. Assuming the same biosynthetic origin with **6**, the absolute configuration of **7** could be determined.

Table 1
Cytotoxicity data of partial compounds.

Compd.	IC_{50} (μmol/L)					
	MGC803	HepG2	MDA-MB-231	MCF-7	Bel-7402	HeLa
1	10.6 ± 0.65	17.1 ± 0.12	38.9 ± 1.24	26.6 ± 0.62	13.2 ± 0.32	9.09 ± 0.38
7	2.5 ± 0.21	7.6 ± 0.06	7.9 ± 0.34	6.6 ± 0.43	2.6 ± 0.79	8.3 ± 0.42
10	3.4 ± 0.10	3.2 ± 0.14	11 ± 0.08	6.5 ± 0.05	9.5 ± 0.93	10 ± 0.46
13	0.76 ± 0.06	2.7 ± 0.19	14 ± 0.39	7.4 ± 0.30	3.2 ± 0.74	11 ± 0.55
15	3.7 ± 0.16	9.9 ± 0.36	9.3 ± 0.15	9.6 ± 0.60	1.5 ± 0.85	2.5 ± 0.34
DOX[a]	0.21 ± 0.23	2.2 ± 0.58	6.6 ± 0.63	4.2 ± 0.32	2.3 ± 0.93	0.79 ± 0.22
5-FU[a]	33 ± 1.20	15 ± 2.15	>50	46 ± 1.32	>50	2.8 ± 0.65

[a] Positive control.

The scaffold of perpyrrospirone A (**1**) is unprecedented and formally different from GKK1032s. while, it is interesting to note that the most significant difference between **1** and GKK1032s is the peroxide-bridged 8,9-dioxa-2-azaspiro[4.7]dodecane core. To explain the formation of the framework of **1**, a plausible biosynthetic pathway is proposed as shown in Scheme 1. Compound **1** was the first hirsutellone peroxide biogenetically biosynthesized though PKS-NRPS gene cluster in *Penicillium citrinum* [3d] and derived from GKK1032s, which was obtained as an abundant component. In brief, one acetyl-CoA, eight malonyl-CoA, four SAM and one L-tryosine could afford GKK1032s. The terminal double bond between C-1 and C-2 reacted by epoxidation to give **ii**, which may be the key intermediate. Then, spiro-lactam was conducted by nucleophilic addition between C-1 and C-17 and gave the key intermediate **iv**. Finally, a peroxide-bridged was formed by rare oxidization to give **1**. Isolated hirsutellones (**1**–**5**, **8**–**10** and **12**–**16**) were covered in the plausible biosynthetic pathway as shown in Scheme 1.

The cytotoxic activities of compounds **1**, **6**–**16** against human tumor cell lines (MGC803, HepG2, MDA-MB-231, MCF-7, Bel-7402 and HeLa) were evaluated using MTT method with doxorubicin and 5-fluorouracil as the positive control (Fig. 5A) [19–21]. Compounds **1**, **7**, **10**, **13** and **15** exhibited cytotoxicity against the above six cell lines with IC_{50} values ranging from 0.76 μmol/L to 38.9 μmol/L (Table 1), and compound **7** was selected to further clarify the mechanism of the death of HeLa cell due to its rare adduct structure. The annexin V-FITC and propidium iodide (PI) containing flow cytometric analysis revealed that **7** induced massive cell apoptosis in a dose-dependent manner but no obvious effects on cell cycle (Figs. 5B and C), suggesting that **7** might inhibit the proliferation of Hela cells by inducing apoptosis other than cell cycle inhibition.

In summary, compound **1** with unprecedented 6/5/6/8/5/13/6 oxahexacyclic scaffold and compounds **2** and **3** with rare oxatetracyclic (6/5/6/5) skeleton were discovered from marine-derived *Penicillium citrinum* based on MN. In particular, identification of the perpyrrospirone A (**1**), first example of hirsutellone peroxide, is of great important in the research field of hirsutellone. The proposed biosynthetic routes implied that a novel enzymic-catalyzed peroxide formation reaction may exist in the post modification of hirsutellone. Compounds **1**, **7**, **10**, **13** and **15** exhibited cytotoxicity and **7** induced apoptosis of HeLa cells in a dose-dependent manner after a 48 h treatment. These findings might provide a route to boost the discovery of antitumor leading candidates.

Declaration of competing interest

The authors declare that they have no known competing financial interests or personal relationships that could have appeared to influence the work reported in this paper.

Acknowledgments

This work was funded by the National Natural Science Foundation of China (Nos. 41876189, 81703388), and the National Key R&D Program of China (Nos. 2018YFC1706206, 2019YFC0312504). This work was also supported by the Open Research Fund Program of State Key Laboratory of Bioreactor Engineering and Institute of Regulatory Science.

Supplementary materials

Supplementary material associated with this article can be found, in the online version, at doi:10.1016/j.cclet.2022.05.076.

References

[1] X.W. Li, A. Ear, B. Nay, Nat. Prod. Rep. 30 (2013) 765–782.
[2] Y. Chen, Z. Liu, Y. Huang, et al., J. Nat. Prod. 82 (2019) 1752–1758.
[3] K.C. Nicolaou, S. David, T.R. Wu, W.Q. Zhan, Angew. Chem. Int. Ed. 48 (2009) 6870–6874.
[4] H. Uchiro, R. Kato, Y. Arai, M. Hasegawa, Y. Kobayakawa, Org. Lett. 13 (2011) 6268–6271.
[5] X.W. Li, A. Ear, L. Roger, et al., Chem. Eur. J. 19 (2013) 16389–16393.
[6] M. Ohashi, T.B. Kakule, M.C. Tang, C.S. Jamieson, et al., J. Am. Chem. Soc. 143 (2021) 5605–5609.
[7] Z.G. Liu, W. Li, P. Zhang, et al., Acta Pharm. Sin. B 11 (2021) 3655–3664.
[8] T. Song, M. Chen, Z.W. Ge, et al., J. Org. Chem. 83 (2018) 13395–13401.
[9] X. Qi, X.Q. Li, J. Y, et al., J. Antibiot. 72 (2019) 237–240.
[10] T. Song, M. Tang, H. Ge, et al., Mar. Drugs 17 (2019) 292.
[11] T. Song, M. Chen, W. Chai, et al., Tetrahedron 74 (2018) 884–891.
[12] S.P. Gaudencio, F. Pereira, Nat. Prod. Rep. 32 (2015) 779–810.
[13] J. Watrous, P. Roach, T. Alexandrov, et al., Proc. Natl. Acad. Sci. U. S. A. 109 (2012) 1743–1752.
[14] J.Y. Yang, L.M. Sanchez, C.M. Rath, et al., J. Nat. Prod. 76 (2013) 1686–1699.
[15] A.E.F. Ramos, C. Alcover, L. Evanno, et al., J. Nat. Prod. 80 (2017) 1007–1014.
[16] L.D. Bari, G. Pescitelli, C. Pratelli, D. Pini, P. Salvadori, J. Org. Chem. 66 (2001) 4819–4825.
[17] Z. Mai, G. Ni, Y. Liu, et al., Acta Pharm. Sin. B 8 (2018) 805–817.
[18] Y.P. Sun, L.T. Cui, Q.R. Li, et al., Chin. Chem. Lett. 33 (2022) 516–518.
[19] T. Mosmann, J. Immunol. Methods 65 (1983) 55–63.
[20] Y. Ding, X.J. Zhu, L.L. Hao, et al., Mar. Drugs 18 (2020) 338.
[21] T.A. Halgren, R.B. Murphy, R.A. Friesner, et al., J. Med. Chem. 47 (2004) 1750–1759.